Photoelectron holography of semiconductor interfaces and study of MBE-grown GaAs(111) surfaces by Jianchao Wu

A thesis submitted in partial fulfillment of the requirements for the degree of Doctor of Philosophy in Physics
Montana State University

Abstract:
The microscopic structures and properties of semiconductor surfaces and interfaces are successfully investigated by several different techniques in this thesis.

First, the small cone photoelectron holographic imaging technique, in conjunction with the LEED observation, has been applied to study the interfacial structures of Se/Ge(100)-lx2, Ga/Ge(111)-1x1 and Ge/Si(100)-2xl samples. The results for the Se/Ge(100)-lx2 suggest that two different regions coexist on the surface. One is fully terminated by Se adatoms at bridge sites, and another is half-covered by Se adatoms on the Ge displaced surface. This is the first experiment to determine the atomic structure of Se/Ge(100)-1x2 sample. The results for the GaZGe(111)-1x1 unambiguously show that the Ga atoms occupy both T4 sites and H3 sites. The results for the GeZSi(100)-2x1 clearly indicate that the Ge adsorption displaces the surface Si atoms from the terraces and forms the Ge dimers on the surface. This determination is in agreement with the combined results of the studies by LEEM, LEED and STM [41].

Second, the GaAs(111)A and GaAs(111)B surfaces, prepared by the MBE growth technique, have been studied by HREELS, XPS, UPS and LEED. The MBE growth with Si-doping produces a p-type semiconductor for GaAs(111)A and a n-type for GaAs(111)B, and both surfaces have the same 2x2 reconstruction. The HREELS results from the clean GaAs(111)A and GaAs(111)B surfaces show the Fuchs-Kleiwer surface optical phonon energy at 35.5 meV, but different plasmon-excitation features. Following atomic hydrogen exposure, both As-H and Ga-H stretching modes are observed on the GaAs(111)B surface, while only Ga-H stretching mode appears in the HREELS spectra of GaAs(111)A surface, which can be explained by the Ga-vacancy buckling model of GaAs(111)A[48]. The hydrogen disruption is observed on the GaAs(111)B surface, but it does not take place on the GaAs(111)A surface.

PHOTOELECTRON HOLOGRAPHY OF SEMICONDUCTOR INTERFACES AND STUDY OF MBE-GROWN GaAs(111) SURFACES

by

Jianchao Wu

A thesis submitted in partial fulfillment

of the requirements for the degree

of

Doctor of Philosophy

in

Physics

MONTANA STATE UNIVERSITY

Bozeman, Montana

April, 1996

APPROVAL

of a thesis submitted by

Jianchao Wu

This thesis has been read by each member of the thesis committee and has been found to be satisfactory regarding content, English usage, format, citations, bibliographic style, and consistency, and is ready for submission to the College of Graduate Studies.

4/16/96
Date

Gerald D. Lappegus
Chairperson, Graduate committee

Approved for the Major Department

5-1-96
Date

J. Stern
Head, Major Department

Approved for the College of Graduate Studies

5/10/96
Date

R. L. Brown
Graduate Dean

STATEMENT OF PERMISSION TO USE

In presenting this thesis in partial fulfillment of the requirements for a doctoral degree at Montana State University-Bozeman, I agree that the Library shall make it available to borrowers under rules of the Library. I further agree that copying of this thesis is allowable only for scholarly purposes, consistent with "fair use" as prescribed in the U.S. Copyright Law. Requests for extensive copying or reproduction of the thesis should be referred to University Microfilms International, 300 North Zeeb Road, Ann Arbor, Michigan 48106, to whom I have granted "the exclusive right to reproduce and distribute my dissertation in and from microform along with the non-exclusive right to reproduce and distribute my abstract in any format in whole or in part."

Signature Jianchao Wu

Date 4-12-96

DEDICATED TO WEILING, PHILIP, LINSEN

AND MY PARENTS

ACKNOWLEDGMENTS

I am very grateful to my thesis advisor, Dr. Gerald J. Lapeyre. His guidance and support throughout past six years enabled me to successfully complete this work. Thank you Jerry!

I would like to thank Dr. James R. Anderson for the advice and support to my training in surface science and experimental aspect of this work. His reading and correcting this thesis is especially appreciated. The author also acknowledges Dr. Cliff Olson at Synchrotron Radiation Center (SRC) for the valuable advice and assistance regarding the monochromators and other experimental apparatus. I would also like to thank Dr. J. Schaefer for his guidance during the early stage of HREELS work. The author would also like to thank the other committee members, Dr. John Hermanson, Dr. Richard Smith and Dr. George Tuthill, for their comments regarding the improvement of this thesis.

The author would like to thank Dr. Huasheng Wu, whose advice and support have been especially valuable. I would also like to thank Dr. Hong Yu. I learned a lot of vacuum techniques in working with him. The author is very grateful to Dr. Mary Keeffe and Cui Chen for their great help and contribution in the experimental setup and data collection at SRC. I would also like to thank the secretarial and technical staff at the MSU Physics Department for their assistance and support.

Finally, a warm thank goes to my wife, Weiling, for her loving care of our little children while working as a full-time engineer, great contribution and sacrifices to our family.

TABLE OF CONTENTS

LIST OF TABLES

LIST OF FIGURES

ABSTRACT

The microscopic structures and properties of semiconductor surfaces and interfaces are successfully investigated by several different techniques in this thesis.

First, the small cone photoelectron holographic imaging technique, in conjunction with the LEED observation, has been applied to study the interfacial structures of Se/Ge(100)-1x2, Ga/Ge(111)-1x1 and Ge/Si(100)-2x1 samples. The results for the Se/Ge(100)-1x2 suggest that two different regions coexist on the surface. One is fully terminated by Se adatoms at bridge sites, and another is half-covered by Se adatoms on the Ge displaced surface. This is the first experiment to determine the atomic structure of Se/Ge(100)-1x2 sample. The results for the Ga/Ge(111)-1x1 unambiguously show that the Ga atoms occupy both T_4 sites and H_3 sites. The results for the Ge/Si(100)-2x1 clearly indicate that the Ge adsorption displaces the surface Si atoms from the terraces and forms the Ge dimers on the surface. This determination is in agreement with the combined results of the studies by LEEM, LEED and STM [41].

Second, the GaAs(111)A and GaAs(111)B surfaces, prepared by the MBE growth technique, have been studied by HREELS, XPS, UPS and LEED. The MBE growth with Si-doping produces a p-type semiconductor for GaAs(111)A and a n-type for GaAs(111)B, and both surfaces have the same 2x2 reconstruction. The HREELS results from the clean GaAs(111)A and GaAs(111)B surfaces show the Fuchs-Kleiwer surface optical phonon energy at 35.5 meV, but different plasmon-excitation features. Following atomic hydrogen exposure, both As-H and Ga-H stretching modes are observed on the GaAs(111)B surface, while only Ga-H stretching mode appears in the HREELS spectra of GaAs(111)A surface, which can be explained by the Ga-vacancy buckling model of GaAs(111)A[48]. The hydrogen disruption is observed on the GaAs(111)B surface, but it does not take place on the GaAs(111)A surface.

CHAPTER 1

INTRODUCTION

The microscopic structures and properties of semiconductor surfaces and interfaces are a major and fundamental field of study in the solid state physics. For the determination of surface structures, the photoelectron holographic imaging technique has drawn a lot of attention in the past few years. Unlike conventional diffraction measurements, where a proposed structure model is iteratively improved to obtain a best fit to the experimental data using a variety of adjustable parameters, the holographic approach permits direct calculation from the raw data without approximation or adjustable parameters and thus provides unambiguous, unique three-dimensional images of the surface and interface atomic structures. The first part of this thesis reports an investigation of the interface structures by the photoelectron holographic imaging technique. The second part will present high-resolution electron energy-loss spectroscopy (HREELS), ultra-violet photoelectron spectroscopy (UPS), x-ray photoelectron spectroscopy (XPS) and low-energy electron diffraction (LEED) studies of GaAs(111)A and GaAs(111)B surfaces grown by the Molecular Beam Epitaxy (MBE).

Motivation of the Present Work and Structure of the Thesis

The atomic structure of an adatom layer formed on the Ge and Si surfaces is of great interest in both surface research and practice because Si and Ge are heavily used semiconductors, and much effort has been used to determine these structures by various kinds of techniques. The purpose of the first part of the present work is to apply the small-cone photoelectron holography technique to determine some adsorbate structures on Si and Ge surfaces, since this method can effectively reveal the three-dimensional images of surface and interface structures without any assumption of structure model.

Over recent years there has been a great increase in interest in the studies of polar surfaces of GaAs(111) due to their technological applications, such as the development of novel electro-optical devices and low-threshold-current lasers [16, 17]. Thus, it is necessary to grow device-quality surfaces of GaAs(111) by MBE and also understanding of their electronic properties. However, most work on the GaAs(111)A and GaAs(111)B surfaces is performed on the sputtered/annealed surfaces. The facility in the CRISS (Center for Research in Surface Science) lab, Physics Department, Montana State University-Bozeman enables us to grow GaAs(111)A and GaAs(111)B surfaces with MBE , transfer the samples into the analysis chamber without exposure to air, and perform the HREELS, XPS, UPS and LEED studies. It would be very profitable to carry out the study on the MBE-grown surfaces and compare the results obtained from the surfaces produced by these two different techniques.

The thesis is organized as follows. Chapter 2 describes the photoemission phenomenon, the principle of photoelectron diffraction and holography, and the small-cone transform. Chapter 3 describes the experimental equipment, setup and procedures, sample preparation, and the data acquisition and analysis of photoelectron holography. Chapter 4 introduces the instrumentation and experimental procedures for the studies of MBE-grown GaAs(111) surfaces. In Chapter 5, we focus on the photoelectron holographic results and discussion for Se/Ge(100)-1x2, Ga/Ge(111)-1x1, and Ge/Si(100)-2x1 samples. Chapter 6 presents the studies of MBE-grown GaAs(111)A and GaAs(111)B surfaces with HREELS, XPS, UPS and LEED techniques. Chapter 7 summarizes the thesis.

Photoelectron Diffraction and Holography

Photoelectron diffraction occurs when a photoemitted electron finds more than one path into a photoelectron detector. One path is provided by direct propagation from the emitting atom (emitter) to the detector (reference wave), while additional paths are available when the photoelectron scatters elastically from nearby atoms (scatterers). Liebsch [1] suggested that photoelectron diffraction could be observed from adsorbates on a surface and that the interference pattern would contain information about the geometry of atoms surrounding the photoemitting adsorbates on surfaces. In 1986, Szoke [2] pointed out that the two-dimensional photoelectron diffraction pattern is a hologram which can be reconstructed to create an image of the three-dimensional crystal structure of a solid surface. The first

experimental work based on this single-energy photoelectron holography technique was performed by Harp *et al* [3] on Cu(100), and it confirmed this phenomenon. Since then, many measurements and calculations [4-6] have been made to determine surface structures. However, all the results showed twin images (spurious maximum intensity at the position inverted about the emitter from the real atom position), as well as poor accuracy in determining the atom position and large artifacts.

In 1992, Tong, *et al* [7] introduced the technique of energy-dependent photoelectron holography, in which the energy-dependent diffraction curves are obtained by measuring the photoelectron energy distribution curve (EDC) over a range of photon energies for a set of emission angles. Then the spectra are inverted with respect to the wave number and summed in real space to obtain the image function. This approach would eliminate the twin image, reduce background noise, as well as give more accurate measurements of atom positions. The first experiment with using this new technique was made by Wu *et al* on the Si(111) $\sqrt{3}$ x $\sqrt{3}$ -Al surface with impressive results in 1993 [8]. In 1994, Wu *et al* proposed the small-cone method to significantly reduce the artifacts and improve the quality of the image[9]. Since then, quite a few experimental results[10-12] have proved this new imaging technique to be very effective in determining the surface and interface structures.

Study of MBE-grown GaAs(111) Surfaces

The III-V compound semiconductors have ordinarily been grown on (100) oriented substrates, because high quality epitaxial layers can be grown under a wide range of growth conditions by MBE. However, over recent years there has been a great increase in interest in the growth on GaAs(111) substrates [13-15]. There are two kinds of GaAs(111) surfaces: GaAs(111)A and GaAs(111)B. If the surface is Ga-terminated, it is called GaAs(111)A. If the surface is As-terminated, it is called GaAs(111)B. The special properties of the (111) surface suggest the possibility of fabricating novel electro-optical devices with strong piezoelectrically generated internal electric fields, and low-threshold-current lasers [16, 17]. High quality expitaxial films on GaAs(111) substrates and the understanding of their surface structure and electronic characteristics are crucial for turning this possibility into reality.

The HREELS technique is a very surface sensitive tool for studying the electronic structures of compound semiconductor surfaces, in particular vibrations of adsorbed gases, such as hydrogen. In addition, XPS (excitation photon energy $h\nu$=151.4eV) spectra provide surface stoichiometry information, the UPS spectra show the valence-band features, while LEED exhibits the surface reconstruction patterns. Thus, HREELS, in conjunction with XPS, UPS and LEED, is very a fascinating technique to study semiconductor surfaces as well as their interaction with hydrogen.

CHAPTER 2

PRINCIPLES OF PHOTOELECTRON HOLOGRAPHY

Angular Resolved Photoemission

The most powerful experimental tools for probing the electronic structure of solids are to be found in the area of photoelectron spectroscopy. An incoming photon with sufficient energy hν is incident upon the surface of a solid and generates the photoelectrons emitted from the sample as shown in Fig. 1.

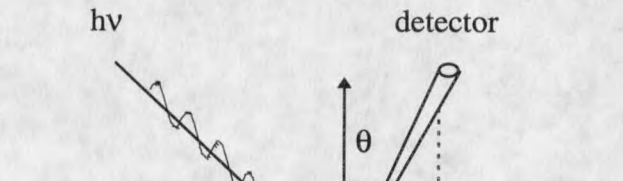

Fig. 1. The photoemission phenomenon. The direction of photoelectrons is defined by the polar angle θ and azimuthal angle φ.

Photoemission spectra are interpreted for most practical purposes within the single-particle approximation. That is, the energy of the photoexcited electron can be written as $E_K=h\nu-E_b-\Phi_w$ where E_b is the binding energy of core-level and Φ_w is the work function of the sample(see Fig. 2).

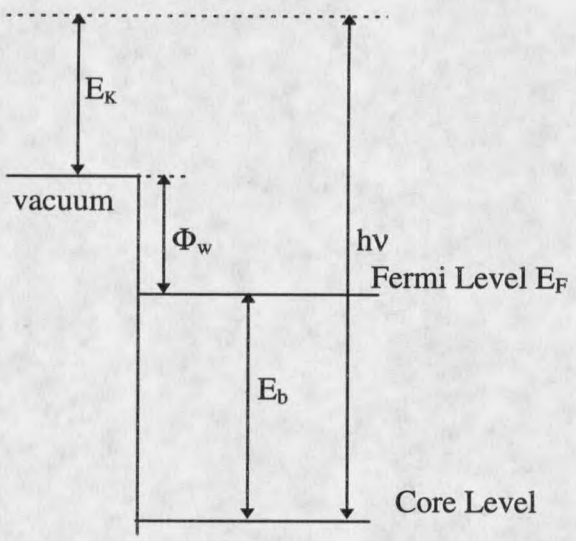

Fig. 2. Energy-level diagram for photoemission process.

In angle-resolved photoemission, if one has measured the kinetic energy of a photoelectron, and also its direction of propagation, one has automatically measured its momentum or wave vector **K** since $E = \hbar^2 K^2/2m$. This follows from the energy conservation and the conservation of wave vector parallel to the surface.

$$\mathbf{K}_{//} = \mathbf{k}_{//} \qquad (2.1)$$

where $\mathbf{K}_{//}$ is the parallel component of the external electron wave vector, and $\mathbf{k}_{//}$ is the parallel component of the electron wave vector inside the sample. The conservation of wave vector in the normal direction breaks down due to the potential barrier at the surface. From the energy conversation,

$$E(k) = E(K) + V_{in} \tag{2.2}$$

where V_{in} is called the inner potential or the surface potential barrier [18], $E(K) = \hbar^2K^2 / 2m$ is the kinetic energy of a photoelectron outside the sample, and $E(k) = \hbar^2k^2 / 2m$ is the kinetic energy inside the sample. From (2.1) and (2.2), we can get

$$\mathbf{k}_\perp^2 = \mathbf{K}_\perp^2 + 2m_e V_{in} / \hbar^2 \tag{2.3}$$

where m_e is the electron mass. The intensity of the photoemitted electron flux depends upon not only the magnitude of the electron momentum (photoexcitaion cross section), but also the emission direction (photoexcitation angular dependence). Both effects could be described by one function, the photoexcitation factor $F_k(\hat{\mathbf{k}})$, where $\hat{\mathbf{k}}$ is a unit vector in the direction of electron momentum and k is the magnitude of the electron momentum.

Photoexcitation Factor

A polarized photon field can be described as

$$\mathbf{A}(\mathbf{r}, t) = \hat{\varepsilon} A_0 \exp[i(\mathbf{q} \cdot \mathbf{r} - \omega t)] \tag{2.4}$$

where $\mathbf{A}(\mathbf{r}, t)$ is the vector potential of the electromagnetic field, $\hat{\varepsilon}$ is the unit vector in the polarization direction, A_0 is the amplitude of the vector potential, ω is the photon angular frequency, $\mathbf{q}$ ($q = \omega/c = 2\pi/\lambda$) is the photon wave vector and $\mathbf{r}$ is the position vector measured from the center of an atom. The photon energy in our experiments is usually is below 250 eV. That is, the wave length λ is greater than 50 Å. It means $\mathbf{q}\cdot\mathbf{r} \approx a_0/\lambda << 1$, where a_0 is the Bohr radius. Thus, Eq (2.4) can be reduced to

$$\mathbf{A}(\mathbf{r}, t) = \hat{\varepsilon} A_0 \exp[-i\omega t] \tag{2.5}$$

In our experiment, $\hat{\varepsilon}$ is chosen along the z direction.

The one-particle Hamiltonian operator that describes the atom's interaction with the electromagnetic field in first-order perturbation approximation is given by [19]

$$\hat{H}_1 = -\frac{e}{2m_e c}(\hat{P}\cdot\mathbf{A} + \mathbf{A}\cdot\hat{P}) \tag{2.6}$$

where $\hat{P} = \frac{\hbar}{i}\nabla$ is the momentum operator. Then, the transition matrix element can be presented as

$$M_{i,f} = \langle f|\hat{H}_1|i\rangle = -\frac{e}{2m_e c}\int \Psi_f^*(\hat{P}\cdot\mathbf{A} + \mathbf{A}\cdot\hat{P})\Psi_i d\mathbf{r} \tag{2.7}$$

where $|f\rangle$ and $|i\rangle$ are respectively the final and initial states obtained from the unperturbed Hamiltonian $\hat{H}_0 = \frac{\hat{P}^2}{2m_e} + eV(r)$, while $\Psi_f = \langle r|f\rangle$ is the final state eigenfunction and $\Psi_i =$

$\langle r|i\rangle$ is the initial state eigenfunction. With the gauge transformation, we can always choose $\nabla\cdot\mathbf{A}=0$. Thus, in the above integrand, $\hat{P}\cdot\mathbf{A}\Psi_i=\frac{\hbar}{i}\nabla\cdot(\mathbf{A}\Psi_i)=\frac{\hbar}{i}[(\nabla\cdot\mathbf{A})\Psi_i+\mathbf{A}\cdot\nabla\Psi_i]$.

The first term vanishes, and we have $\hat{H}_I=-\frac{e}{m_e c}\mathbf{A}\cdot\hat{P}$. By the commutation rule $\hat{P}=\frac{im_e}{\hbar}[\hat{H}_0,\mathbf{r}]$, the transition matrix element can be further written as

$$M_{i,f}=-\frac{ie}{\hbar m_e c}e^{-i\omega t}\langle f|\hat{\varepsilon}A_0\cdot(\hat{H}_0\mathbf{r}-\mathbf{r}\hat{H}_0|i\rangle=\frac{e}{i\hbar m_e c}(E_f-E_i)e^{-i\omega t}A_0\langle f|\hat{\varepsilon}\cdot\mathbf{r}|i\rangle \quad (2.8)$$

where E_f is the energy of final state, E_i is the energy of initial state and $E_i-E_f=\hbar\omega$. Assuming the angle between $\hat{\varepsilon}$ and $\mathbf{r}$ is θ, then Eq (2.8) is simplified as

$$M_{i,f}=\frac{ie\omega}{m_e c}e^{-i\omega t}A_0\langle f|r\cos(\theta)|i\rangle \quad (2.9)$$

Consider a spinless particle subjected to a spherically symmetric potential. The wave equation is known to be separable in spherical coordinates and the eigenfunctions can be written as [20] $\langle\mathbf{r}|nlm\rangle=R_{nl}(r)Y_l^m(\theta,\phi)$, where the position vector $\mathbf{r}$ is specified by the spherical coordinates r, θ and ϕ, and n stands for the principle quantum number, while l and m are the angular momentum quantum numbers. $M_{i,f}$ can be written as

$$M_{i,f}=\frac{ie\omega}{m_e c}A_0e^{-i\omega t}\int Y_{lm}^*(\theta,\phi)\cos(\theta)\,Y_{l_0m_0}(\theta,\phi)d\Omega\int R_{nl}(r)R_{n_0l_0}(r)r^3dr \quad (2.10)$$

where $d\Omega=\sin(\theta)d\theta d\phi$. By the orthogonality of the spherical harmonics, we will have a non-vanishing transition only if

$$l=l_0\pm1,\quad m=m_0 \quad (2.11)$$

This is called the dipole transition selection rule. Then the photoexcitation factor is defined as [21]

$$F_k(\hat{\mathbf{k}}) = \frac{2m_e}{\hbar^2}\sum_{lm} Y_{lm}(\hat{\mathbf{k}})M_{i,f} \tag{2.12}$$

where $\hat{\mathbf{k}}$ stands for (θ,ϕ). In the simplest case: the initial state is an s state, that is, $m_0=0$, $l_0=0$, then from Eq (2.12) we can get $F_k(\hat{\mathbf{k}}) \propto \cos(\theta)$. It means that the photoexcitation is highest in the polarization direction for the s-state excitation.

If only the photoexcitation effect is considered, then the photoelectron wave function is given by [21]

$$\Psi(\mathbf{k}) = \frac{2m_e}{\hbar^2}\sum_{lm} R_{nl}(r)Y_{lm}(\hat{\mathbf{r}})M_{i,f} \tag{2.13a}$$

$$= \frac{e^{ikr}}{r}F_k(\hat{\mathbf{k}}) \qquad r \to \infty \tag{2.13b}$$

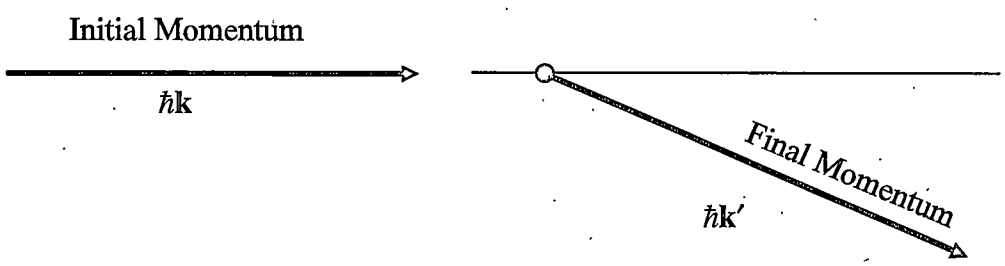

Fig. 3. Initial and final momentum states in scattering.

Atomic Scattering Factor

A photoelectron generally undergoes a number of scatterings before leaving a solid. In quantum mechanics [20], this effect can be described by an atomic scattering factor f(**k**′, **k**), where **k** the initial wave vector and **k**′ is the final wave vector after scattering (see Fig. 3).

For the time-independent scattering process, we assume that the Hamiltonian is written as $\mathbf{H} = \mathbf{H}_0 + \mathbf{V}(\mathbf{r})$, where $\mathbf{H}_0$ stands for the kinetic-energy operator. Then in the first-order perturbation approximation, f(**k**′, **k**) for the outgoing wave is represented as

$$f(\mathbf{k}',\mathbf{k}) = -\frac{4\pi^2 m_e}{\hbar^2}\left\langle \mathbf{k}' \middle| V(\mathbf{r}) \middle| \psi^+ \right\rangle \tag{2.14a}$$

$$= -\frac{4\pi^2 m_e}{\hbar^2}\int d\mathbf{r}' \frac{e^{-i\mathbf{k}'\cdot\mathbf{r}'}}{(2\pi)^{3/2}} V(\mathbf{r}')\left\langle \mathbf{r}' \middle| \psi^+ \right\rangle \tag{2.14b}$$

at large distances. $\langle \mathbf{r}' | \Psi^+ \rangle$ denotes the outgoing scattered wave function. In terms of partial-wave expansion, f(**k**′, **k**) can be written as [20]

$$f(\mathbf{k}',\mathbf{k}) = f_k(\theta) = \frac{1}{k}\sum_{l=0}(2l+1)e^{i\delta_l}\sin\delta_l P_l(\cos\theta) \tag{2.15}$$

where θ is the scattering angle, δ_l is the phase of the outgoing wave and is a function of k, and $P_l(\cos\theta)$ is described as

$$P_l(\cos\theta) = \frac{(-1)^l}{2^l l!}\frac{d^l(1-\cos^2\theta)^l}{d(\cos\theta)^l} \tag{2.16}$$

If only the scattering effect is considered, then the scattered outgoing spherical wave at larger distances can be written as

$$\Psi(r) = \frac{e^{ikr}}{r} f(\mathbf{k}', \mathbf{k}) \qquad (2.17)$$

Photoelectron Diffraction

A photon with energy hν is incident on the surface and ejects a photoelectron from an atom (emitter). Part of the photoelectron wave, called reference wave Ψ_D, will directly propagate into the detector, while the rest of photoelectron wave will be scattered by the neighboring atoms and then go to the detector, called object wave Ψ_S. The reference wave will interfere with the object waves and form a two-dimensional diffraction pattern. This phenomenon is called photoelectron diffraction and is illustrated in Fig. 4.

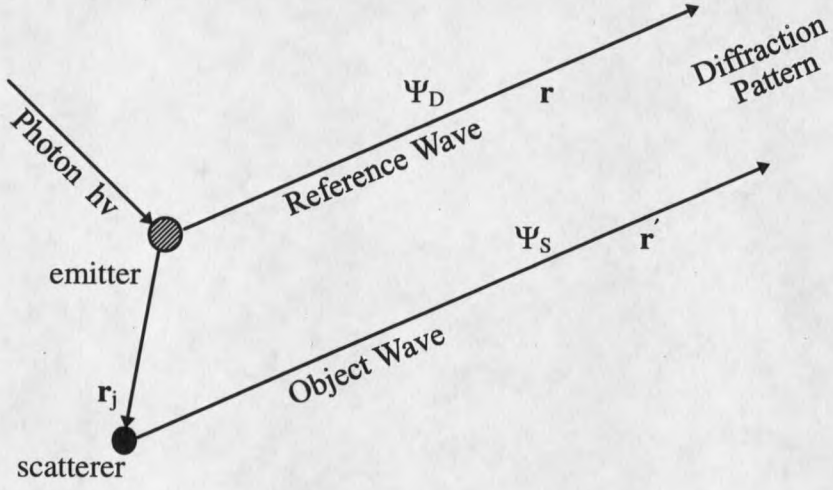

Fig. 4. The phenomenon of photoelectron diffraction.

Only the waves from the same emitter are coherent and can interfere with each other. The waves from different emitters are incoherent. Thus they do not interfere with each other, and their intensities are just added together. Next, it will be shown that the three dimensional images of the surface structures can be reconstructed from the diffraction patterns.

If we place the origin of the coordinate system at atom α, which is the emitter, the photoelectron final wave function at the observation point is given by

$$\psi(\mathbf{k}) = \psi_D(\mathbf{k}) + \psi_S(\mathbf{k}) \tag{2.18}$$

where $\psi_D(\mathbf{k})$ is the reference wave function, $\psi_S(\mathbf{k})$ is the object wave function. From Eq. (2.13), $\Psi_D(\mathbf{k}) = \frac{e^{ikr}}{r} F_k(\hat{\mathbf{k}})$ at large distances. The object wave function is given as

$$\Psi_S(\mathbf{r}') = \Psi_D(\mathbf{r}_j)\frac{e^{ikr'}}{r'} f_k(\hat{\mathbf{k}}\cdot\hat{\mathbf{r}}_j) \tag{2.19}$$

$$\Psi_D(\mathbf{r}_j) = \frac{e^{ikr_j}}{r_j} F_k(\hat{\mathbf{r}}_j) \tag{2.20}$$

From Fig. 4, we can see

$$\mathbf{r}' = \mathbf{r} - \mathbf{r}_j \tag{2.21}$$

Since r and r′ are very large compared to r_j, Eq (2.21) can be written as

$$r' = r(1 - \hat{\mathbf{k}}\cdot\hat{\mathbf{r}}_j) \tag{2.22}$$

Thus, Eq (2.19) becomes

$$\Psi_S(\mathbf{r}') = \frac{e^{ikr_j}}{r_j} F_k(\hat{\mathbf{r}}_j)\frac{e^{ikr - ik\cdot r_j}}{r} f_k(\hat{\mathbf{k}}\cdot\hat{\mathbf{r}}_j) \tag{2.23a}$$

$$= \Psi_D(\mathbf{k})A(\mathbf{k},\mathbf{r}_j)e^{i(kr_j - \mathbf{k}\cdot\mathbf{r}_j)} \tag{2.23b}$$

where

$$A(\mathbf{k},\mathbf{r}_j) = \frac{F_k(\hat{\mathbf{r}}_j)}{F_k(\hat{\mathbf{k}})}\frac{f_k(\hat{\mathbf{k}}\cdot\hat{\mathbf{r}}_j)}{r_j} \tag{2.24}$$

$A(\mathbf{k},\mathbf{r}_j)$ is called the effective scattering factor.

There are more than one atom around the emitter and thus the object wave function is the summation of the scattered waves from each scatterer.

$$\Psi_S(\mathbf{k}) = \Psi_D(\mathbf{k})\sum_j A(\mathbf{k},\mathbf{r}_j)e^{i(kr_j-\mathbf{k}\cdot\mathbf{r}_j)} \tag{2.25}$$

So the final wave function is

$$\Psi(\mathbf{k}) = \Psi_D(\mathbf{k})\left(1+\sum_j A(\mathbf{k},\mathbf{r}_j)e^{i(kr_j-\mathbf{k}\cdot\mathbf{r}_j)}\right) \tag{2.26}$$

Then, the photoelectron diffraction intensity $I(\mathbf{k})$ is written as

$$I(\mathbf{k}) = |\Psi(\mathbf{k})|^2 = \left(\Psi_D(\mathbf{k})+\Psi_S(\mathbf{k})\right)\left(\Psi_D(\mathbf{k})+\Psi_S(\mathbf{k})\right)^*$$

$$= I_0(\mathbf{k})\left(1+\sum_j A(\mathbf{k},\mathbf{r}_j)e^{i(kr_j-\mathbf{k}\cdot\mathbf{r}_j)}+\sum_j A^*(\mathbf{k},\mathbf{r}_j)e^{-i(kr_j-\mathbf{k}\cdot\mathbf{r}_j)}\right.$$

$$\left.+\sum_j\sum_n A(\mathbf{k},\mathbf{r}_j)A^*(\mathbf{k},\mathbf{r}_n)e^{i(kr_j-\mathbf{k}\cdot\mathbf{r}_j)}e^{-i(kr_n-\mathbf{k}\cdot\mathbf{r}_n)}\right) \tag{2.27}$$

Where $I_0 = |\Psi_D(\mathbf{k})|^2$. The last term in Eq. (2.27) can be ignored because of $|A| < 1$. I_0 is the reference wave intensity and does not contain any diffraction information. So we define a normalized hologram function $\chi(\mathbf{k})$ by removing the reference wave as much as possible.

$$\chi(\mathbf{k}) \equiv I(\mathbf{k})/I_0(\mathbf{k}) - 1 \tag{2.28a}$$

$$= \sum_j A(\mathbf{k},\mathbf{r}_j)e^{i(kr_j-\mathbf{k}\cdot\mathbf{r}_j)}+\sum_j A^*(\mathbf{k},\mathbf{r}_j)e^{-i(kr_j-\mathbf{k}\cdot\mathbf{r}_j)} \tag{2.28b}$$

This hologram function $\chi(\mathbf{k})$ contains just the oscillating (interference) part of the hologram.

The experimental energy-dependent photoelectron diffraction spectra are obtained by measuring the core-level peak intensities over a range of photon energies and a set of emission